Stackplots

Giulia Maineri

Università degli studi di Milano

March 2022

Table of Contents

Selections: mll-all, nobjets, MET-A, mT-all, metsig-all

- mll-all: no selections in leptons invariant mass
- nobjets: b-veto, selection of events without b-jets
- MET-A: selection of A region, at high MET and high $\Delta\Phi(\vec{E}_T^{miss}, \vec{p}_T^{\gamma ll})$
- mT-all: no selections in transverse mass
- metsig-all: no selections in MET significance

Missing transverse energy, MET $\vec{E}_T^{miss}$

$$\vec{E}_T^{miss} = -\left[\sum_e \vec{p}_T^{(e)} + \sum_\mu \vec{p}_T^{(\mu)} + \sum_\gamma \vec{p}_T^{(\gamma)} + \sum_\tau \vec{p}_T^{(\tau)} + \sum_{jet} \vec{p}_T^{(jet)} + \sum_x \vec{p}_T^{(x)}\right]$$

Figure 1: eeγ channel

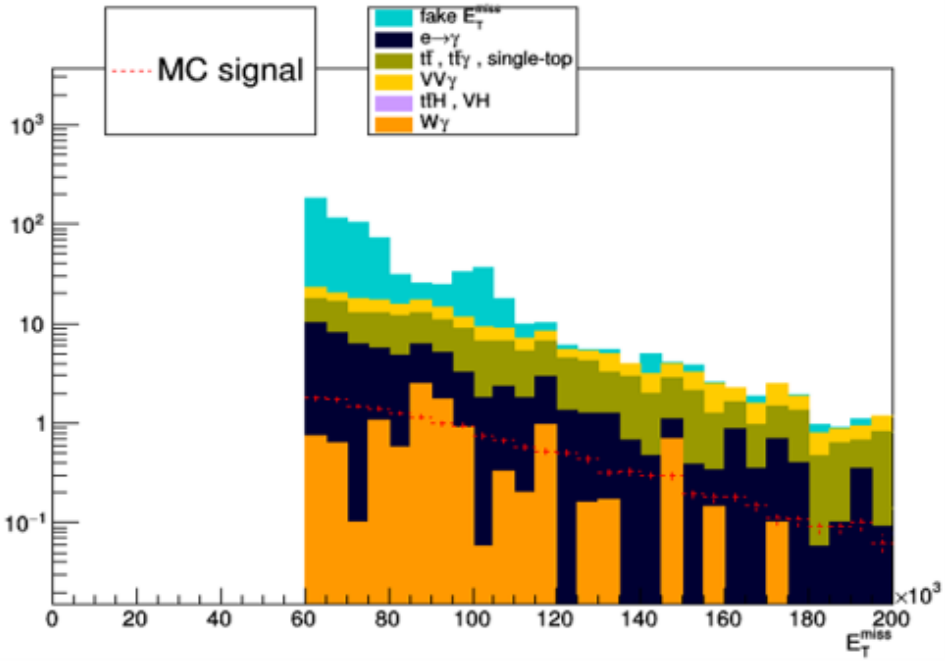

Figure 2: $\mu\mu\gamma$ channel

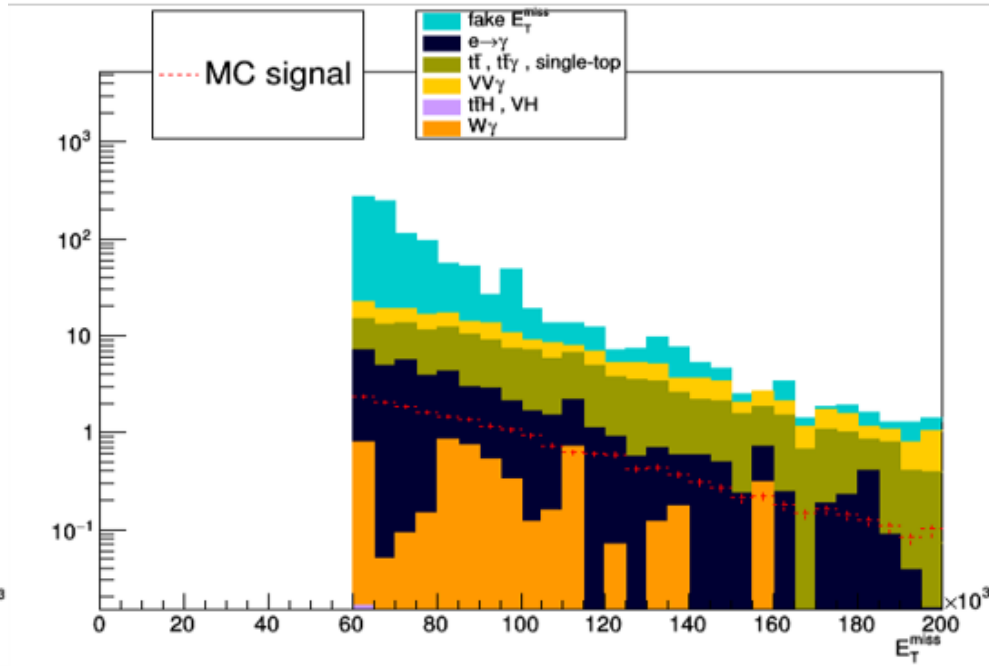

Missing transverse energy, MET $\vec{E}_T^{miss}$

Notes

- There are less $W\gamma$ events in $\mu\mu\gamma$ channel
- Fake MET decrease faster than signal at higher values of MET
- There is the 60 GeV cut in MET that defines SR

MET significance $\sigma_{E_T^{miss}}$

$$sig = \frac{E_T^{miss}}{\sigma_{E_T^{miss}}}$$

Figure 3: eeγ channel

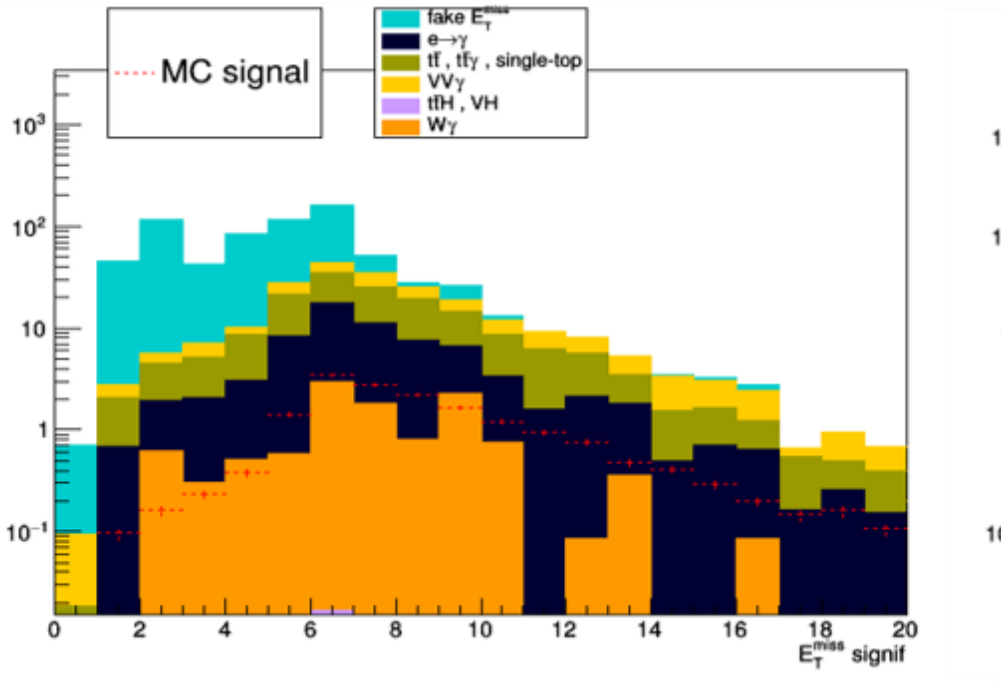

Figure 4: $\mu\mu\gamma$ channel

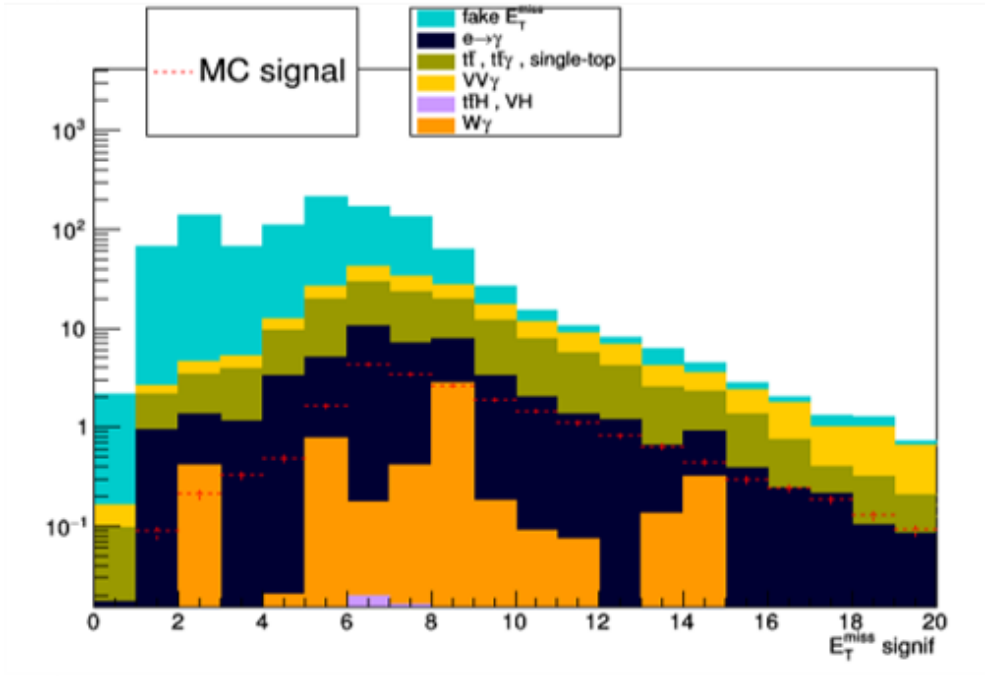

$\Delta\Phi(\vec{E}_T^{miss}, \vec{p}_T^{closest})$

Figure 5: eeγ channel

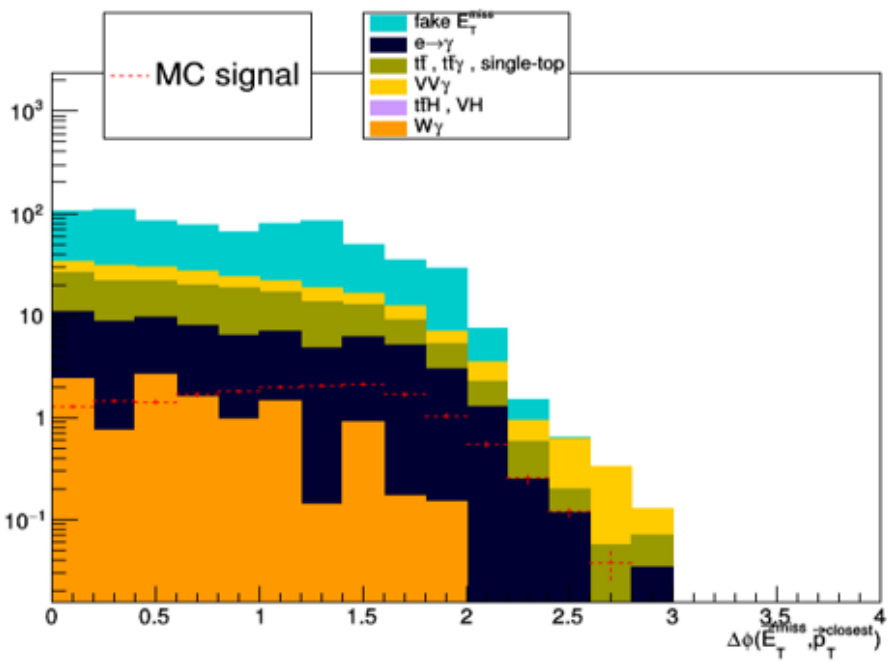

Figure 6: $\mu\mu\gamma$ channel

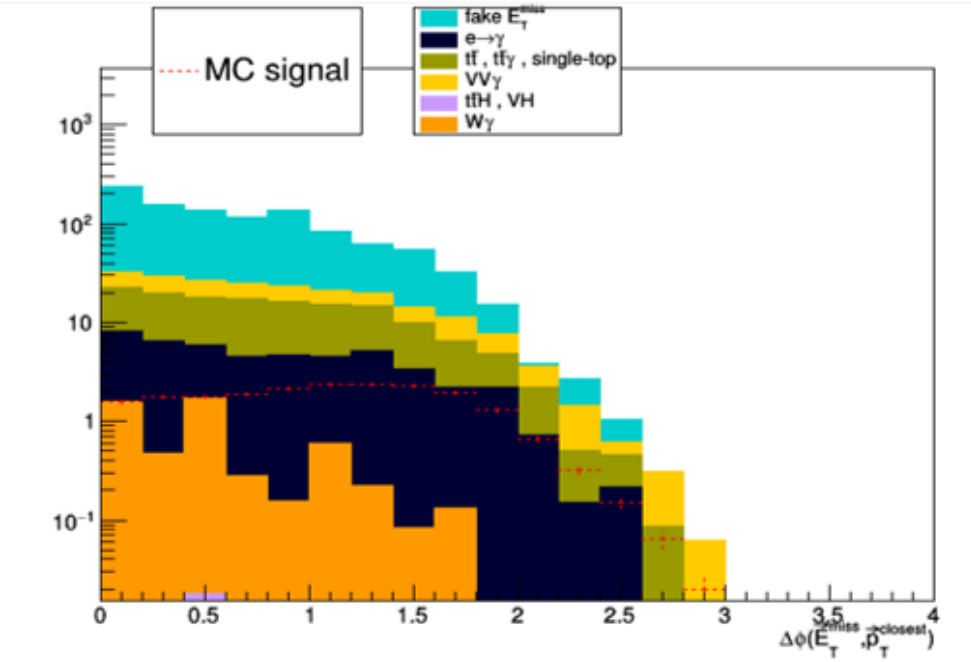

$\Delta\Phi(\vec{E}_T^{miss}, \vec{p}_T^{closestjet})$

Figure 7: eeγ channel

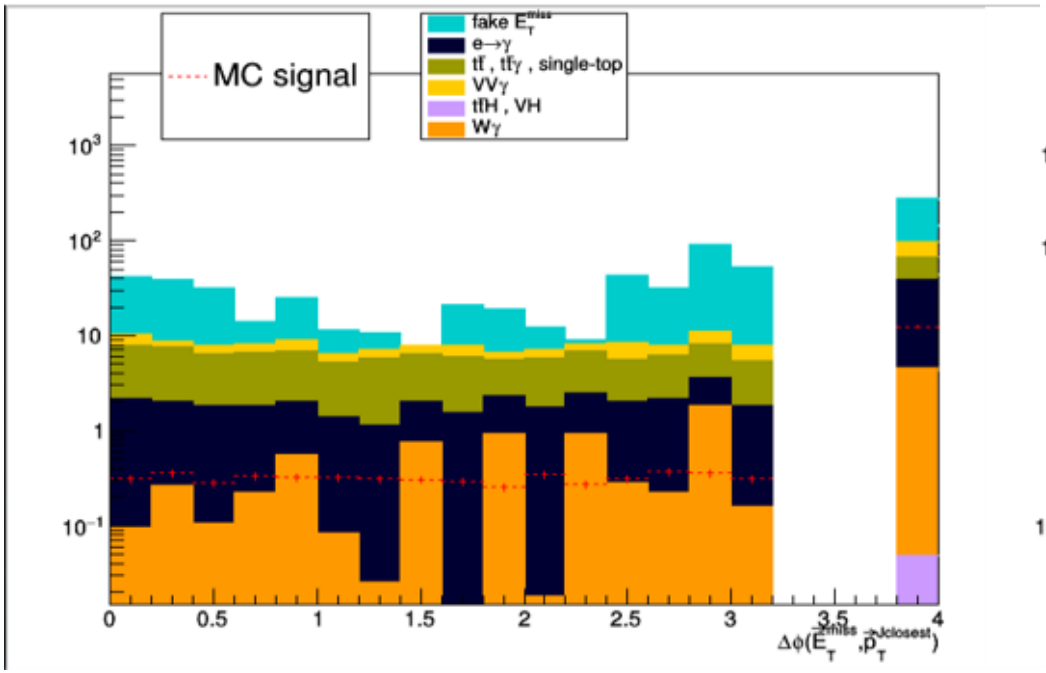

Figure 8: $\mu\mu\gamma$ channel

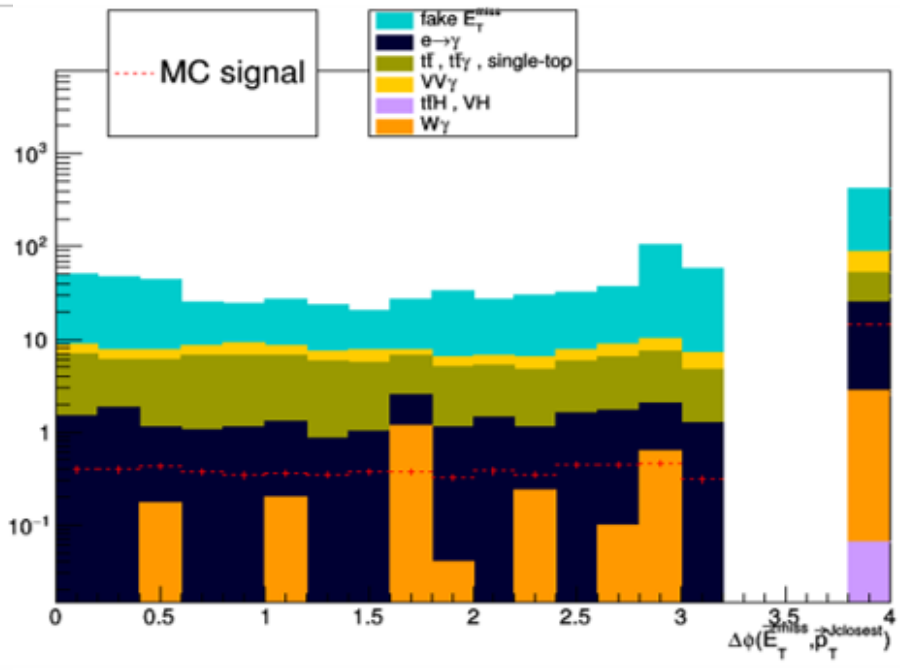

$\Delta\Phi(E_T^{miss}, \sum \vec{p}_T^{jets})$

Figure 9: eeγ channel

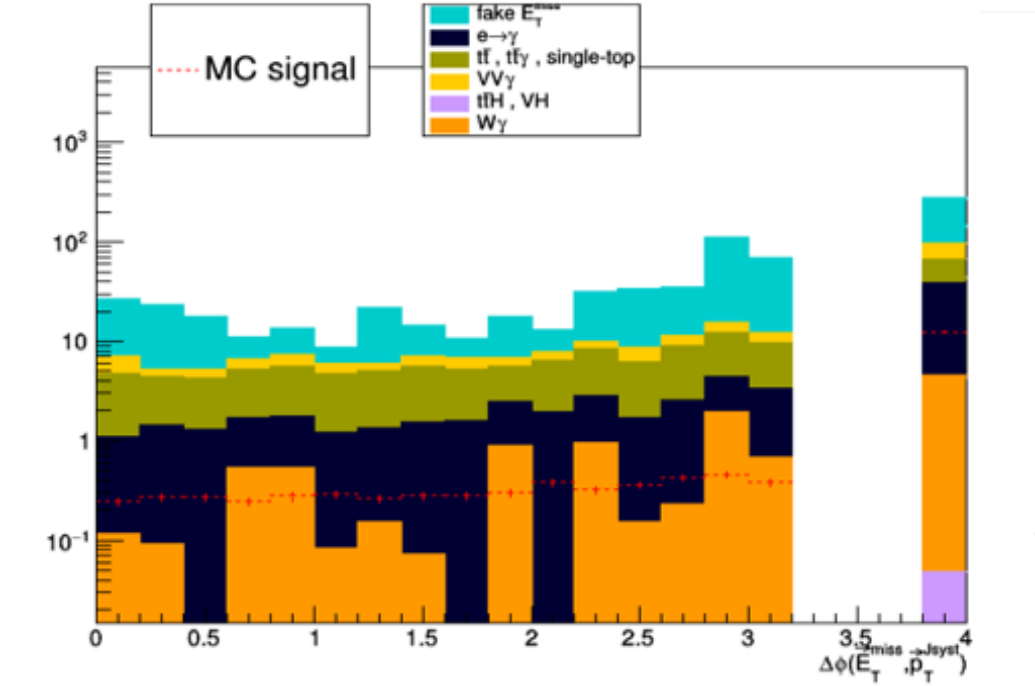

Figure 10: $\mu\mu\gamma$ channel

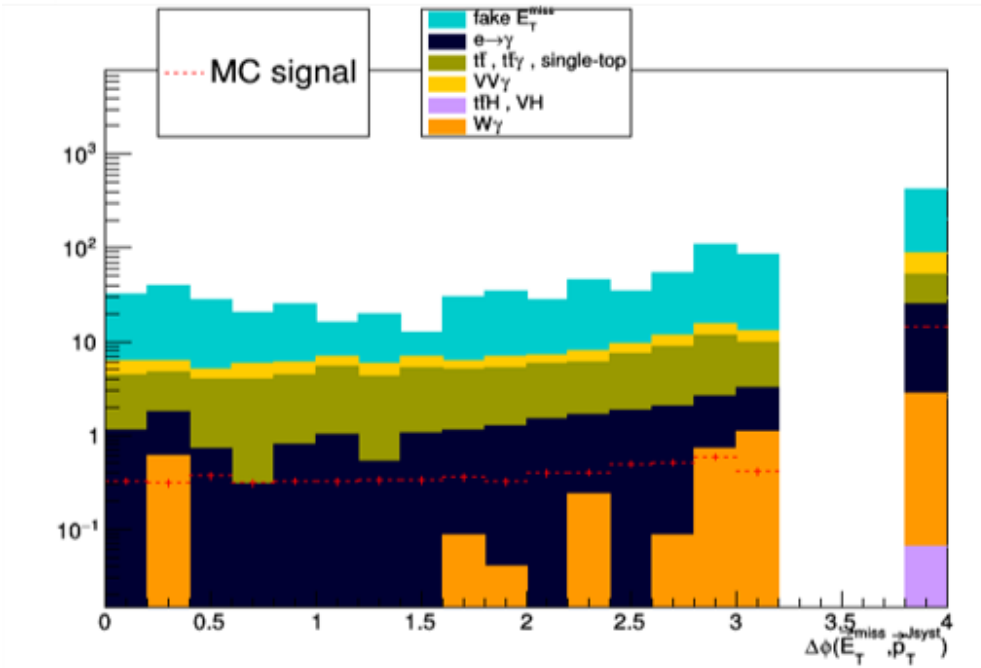

$\Delta\Phi(\vec{E}_T^{miss}, \vec{p}_T^{\gamma ll})$

Figure 11: eeγ channel

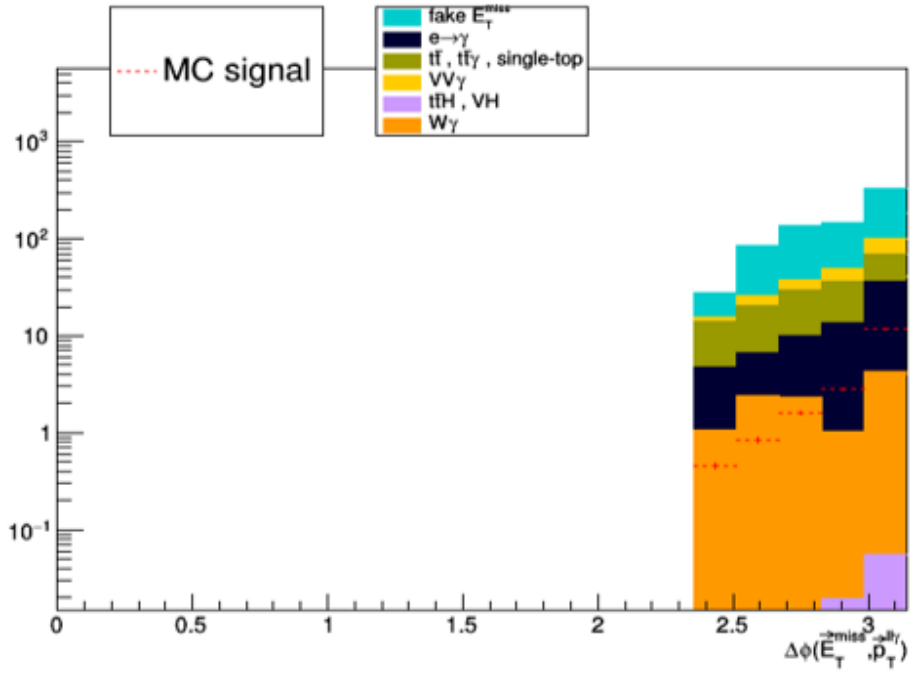

Figure 12: $\mu\mu\gamma$ channel

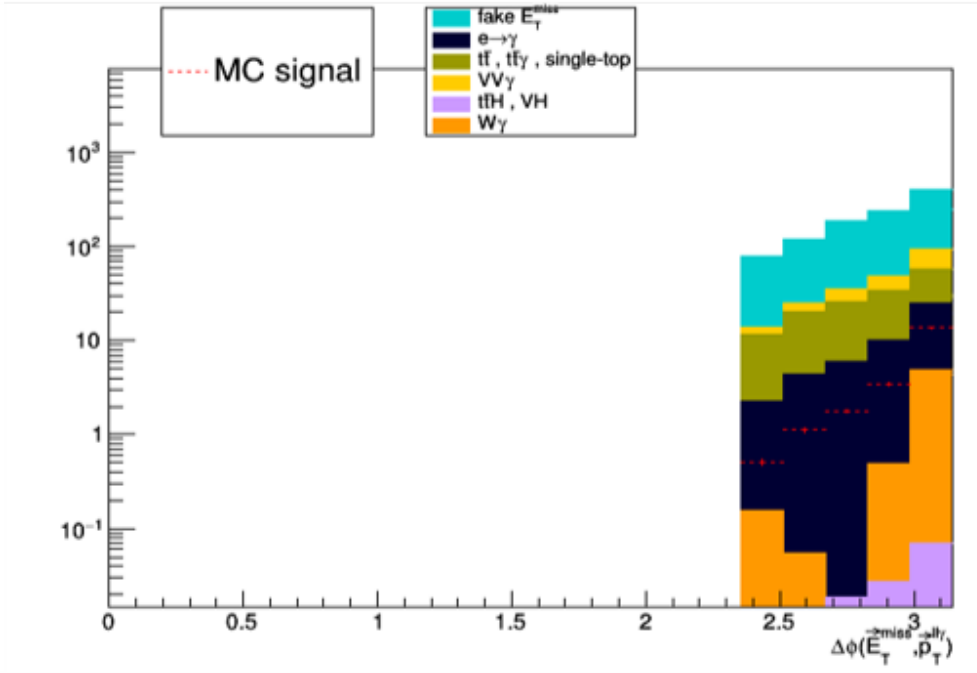

$\Delta\Phi(\vec{E}_T^{miss}, \vec{p}_T^{\gamma ll})$ (selection MET-SR)

Figure 13: eeγ channel

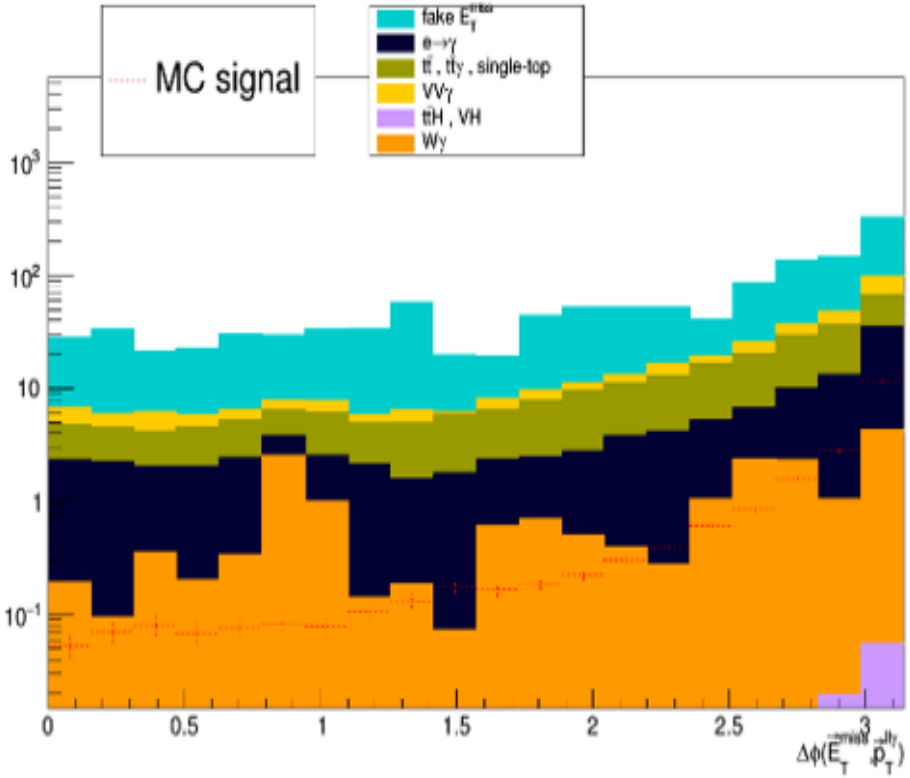

Figure 14: $\mu\mu\gamma$ channel

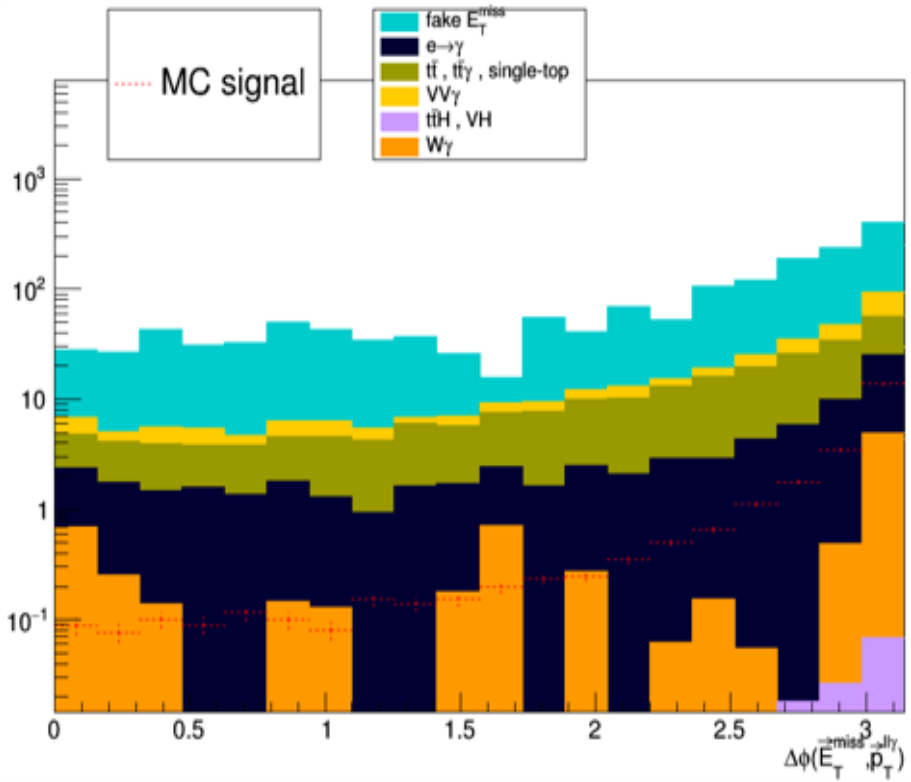

$\Delta\Phi(\vec{E}_T^{miss}, \vec{p}_T^{closest})$, $\Delta\Phi(\vec{E}_T^{miss}, \vec{p}_T^{closestjet})$, $\Delta\Phi(\vec{E}_T^{miss}, \sum \vec{p}_T^{jets})$, $\Delta\Phi(\vec{E}_T^{miss}, \vec{p}_T^{\gamma ll})$

Notes

- Angle between MET and the closest object is often smaller than $\pi/2$
- When there are problems in finding the closest jet, angle is set to impossible value, i. e. 4
- Angle between MET and the closest jet momentum and angle between MET and the sum of all jets momenta seem not to help in discriminating signal and background
- There is the 2.4 cut in $\Delta\Phi(\vec{E}_T^{miss}, \vec{p}_T^{\gamma ll})$ that defines SR
- With a MET-SR selection, i. e. no cut at 2.4, the faster decrease of $\Delta\Phi(\vec{E}_T^{miss}, \vec{p}_T^{\gamma ll})$ is observed, contrasting with background's flat distribution

$$\eta = -\ln\left(\tan\left(\frac{\theta}{2}\right)\right)$$

Figure 15: eeγ channel

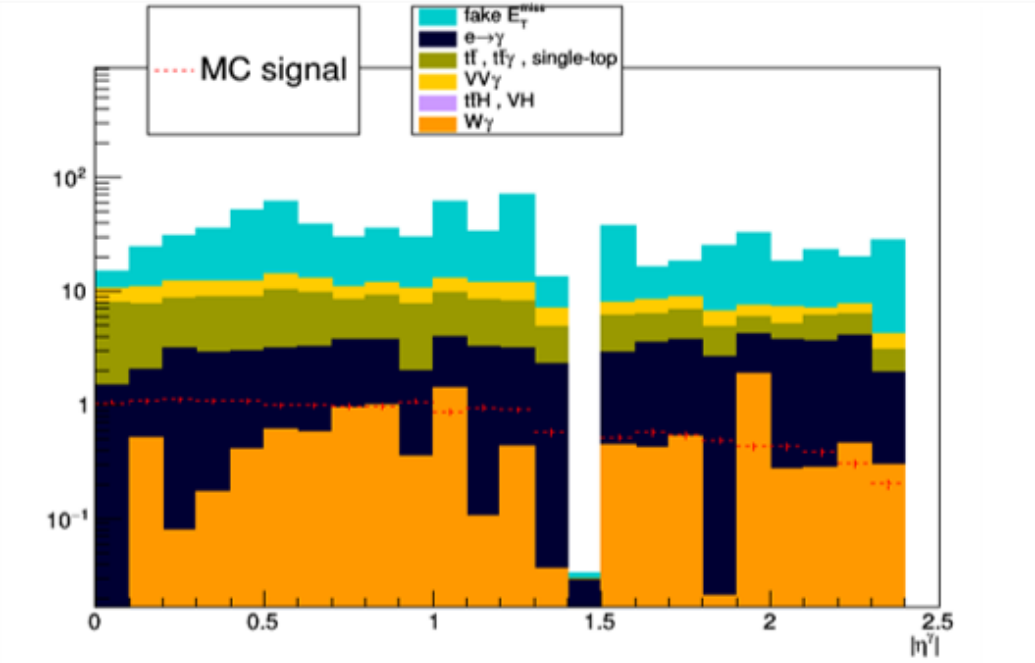

Figure 16: $\mu\mu\gamma$ channel

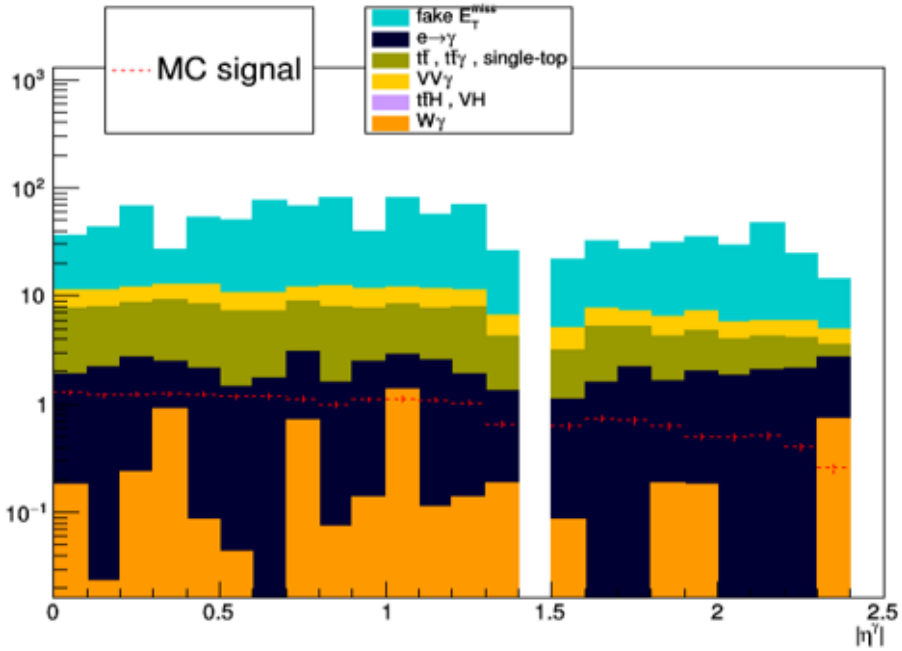

Notes

- A lack of values is observed in the interval $\eta_\gamma = [1.37, 1.52]$ due to a crack region caused by poor performance of detectors (calorimeters)
- The presence of value in the $ee\gamma$ channel can be related to binning effect and/or to differences between η and η_2,as crack region is defined on the latter.

Transverse mass

$$m_T = \sqrt{2p_T^{\gamma} E_T^{miss}(1 - cos(\Phi^{\gamma} - \Phi^{E_T^{miss}}))}$$

Figure 17: eeγ channel

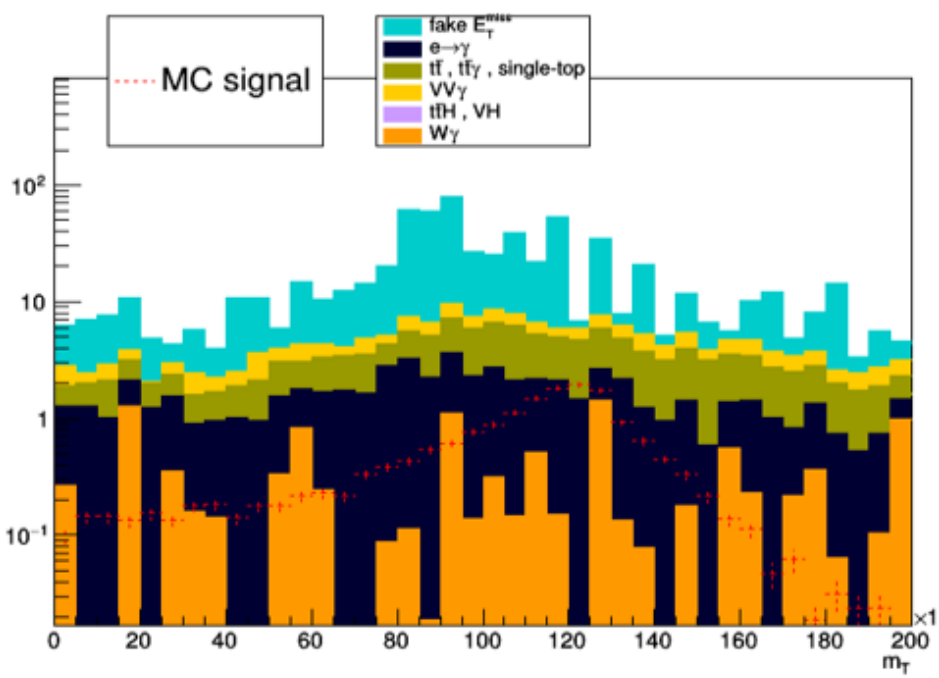

Figure 18: $\mu\mu\gamma$ channel

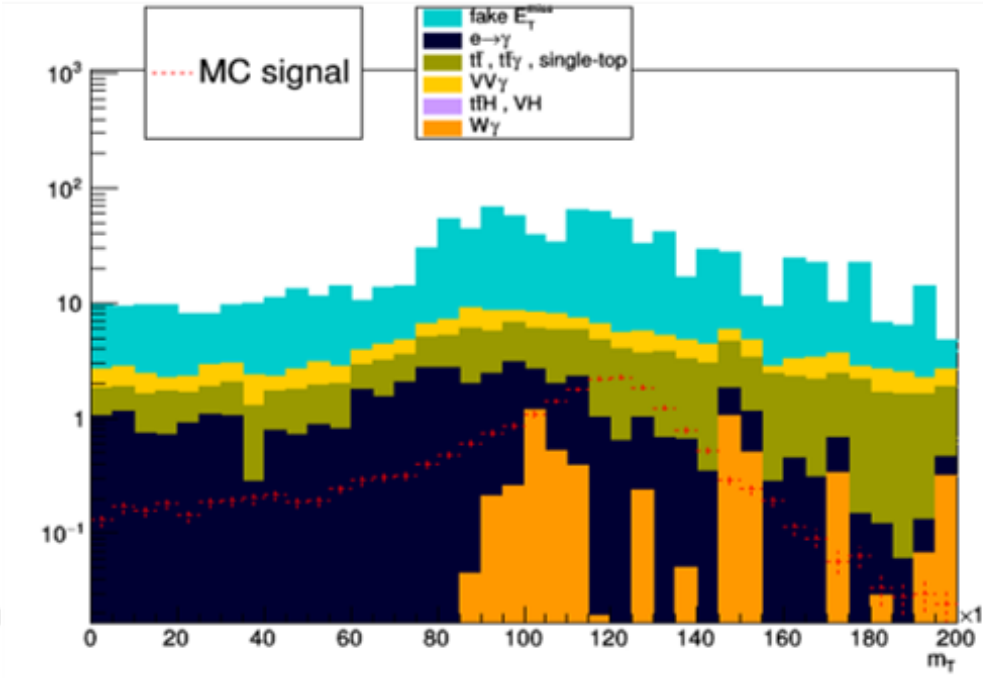

Invariant mass m_{ll}

$$m_{ll} = \sqrt{(E_{l1} + E_{l2})^2 - (\vec{p}_{l1} + \vec{p}_{l2})^2}$$

$$m_{ll} = \sqrt{2p_T^{l1}p_T^{l2}[\cosh(\eta^{l1} - \eta^{l2}) - cos(\Phi^{l1} - \Phi^{l2})]}$$

Figure 19: eeγ channel

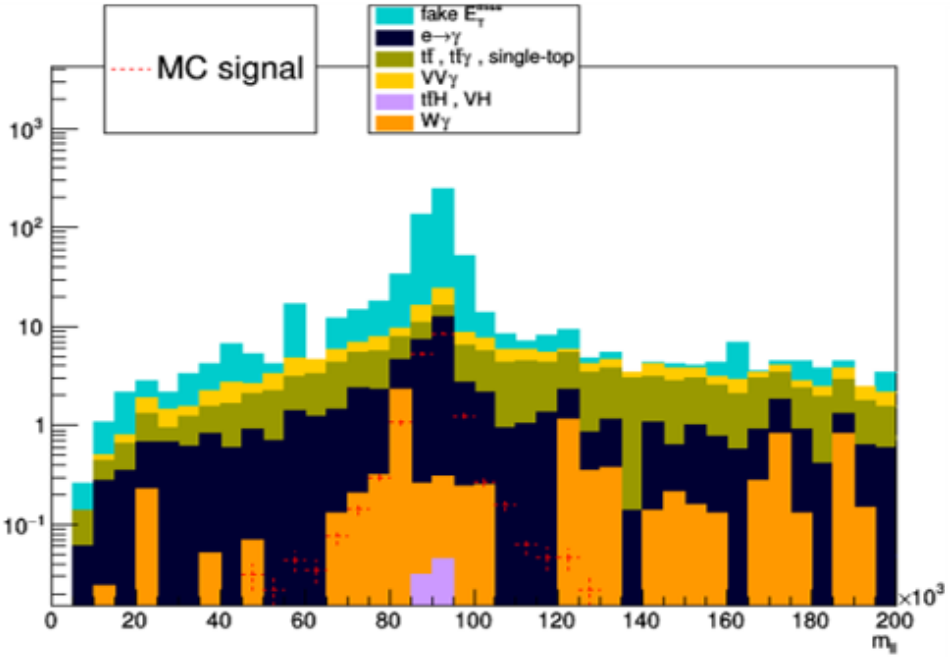

Figure 20: $\mu\mu\gamma$ channel

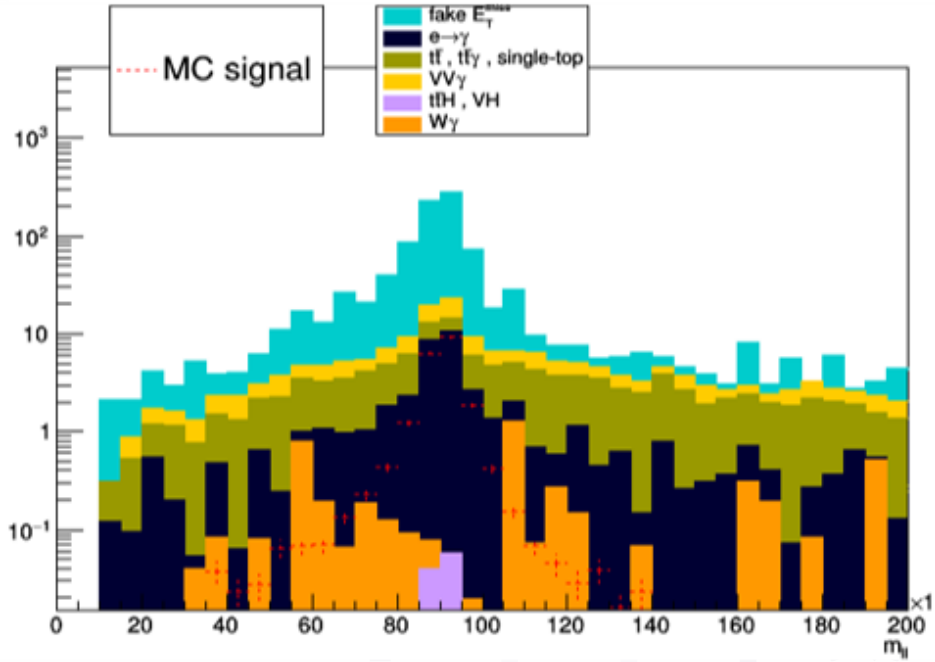

Invariant mass $m_{ll\gamma}$

$$m_{ll\gamma} = \sqrt{(E_{l1} + E_{l2} + E_{\gamma})^2 - (\vec{p}_{l1} + \vec{p}_{l2} + \vec{p}_{\gamma})^2}$$

Figure 21: eeγ channel

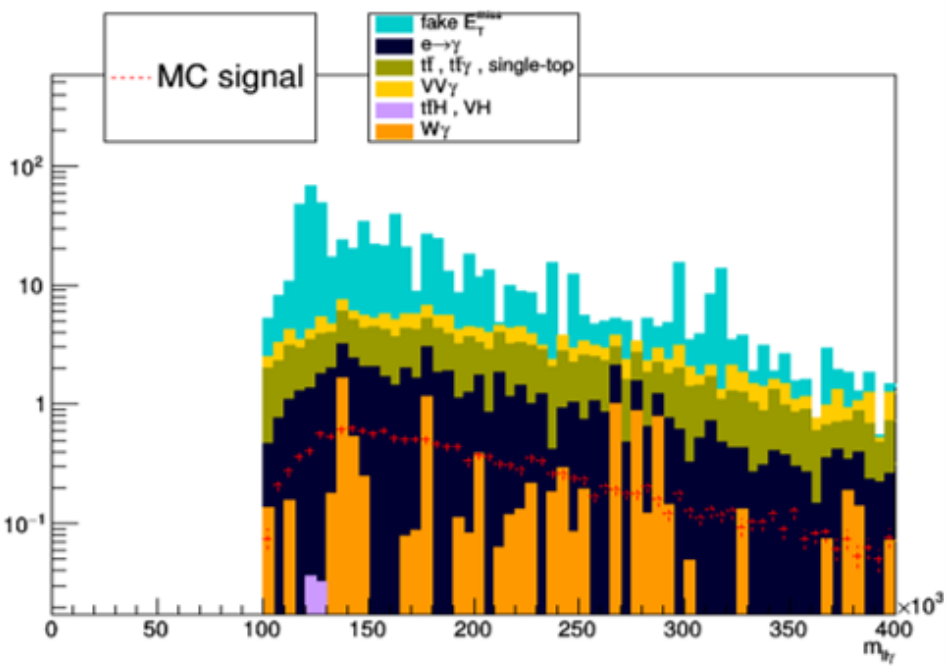

Figure 22: $\mu\mu\gamma$ channel

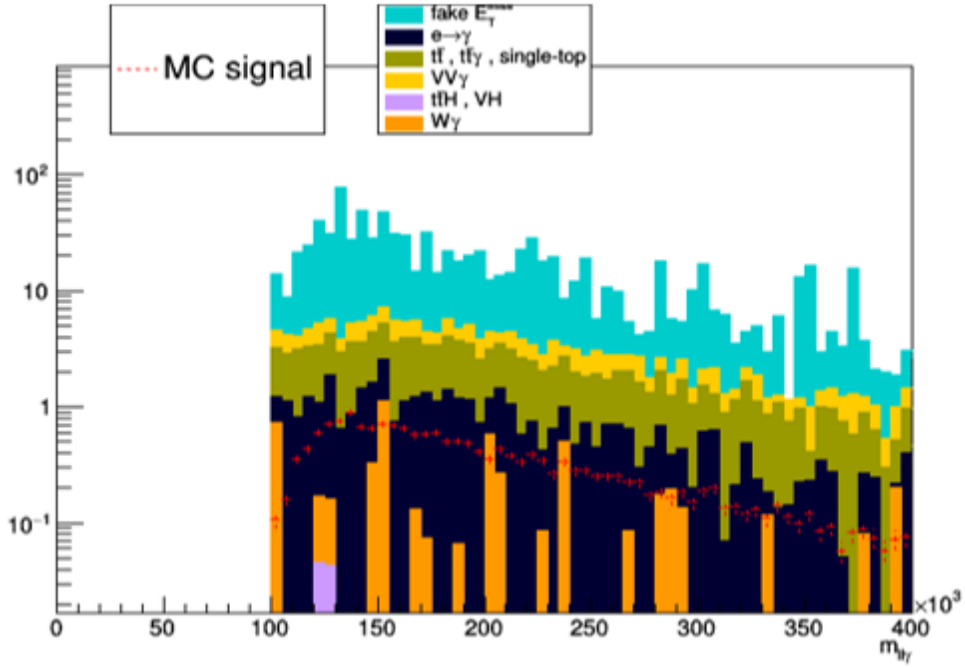

$m_T, m_{ll}, m_{ll\gamma}$

Notes

- Transverse mass seems to be discriminating as there is a peak in signal around $125\,\mathrm{GeV}$, Higgs boson mass, which is not present in background
- A peak is observed in m_{ll} around $90\,\mathrm{GeV}$, which is boson Z mass. This peak is much thinner for signal. Side-bands for background are larger due to the overlap of two processes with the same final state but different mediator: virtual Z boson and virtual photon. A virtual photon can couple with both quarks and leptons as they are charged objects, but not with Higgs boson H which can only couple with massive objects. Invariant mass m_{ll} seems to be a good discriminator.

$m_T, m_{ll}, m_{ll\gamma}$

- A $100\,\mathrm{GeV}$ cut in $m_{ll\gamma}$ has been done in order to avoid Z boson three-bodies decays which produce two leptons and a photon such as signal, but with a lower $m_{ll\gamma}$ as it should be around $90\,\mathrm{GeV}$ for three-bodies decays. In our signal $m_{ll\gamma}$ should be higher as m_{ll} is around $90\,\mathrm{GeV}$.

Transverse momentum balance

$$p_T^{balance} = \frac{p_T^{\gamma+E_T^{miss}}}{p_T^{ll}}$$

Figure 23: eeγ channel

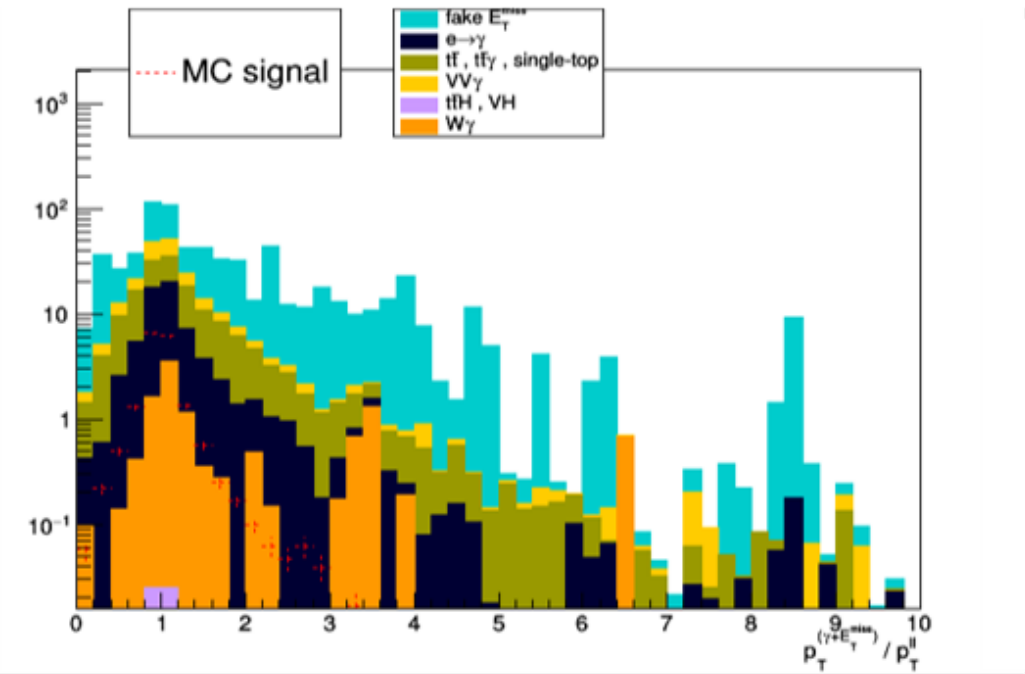

Figure 24: $\mu\mu\gamma$ channel

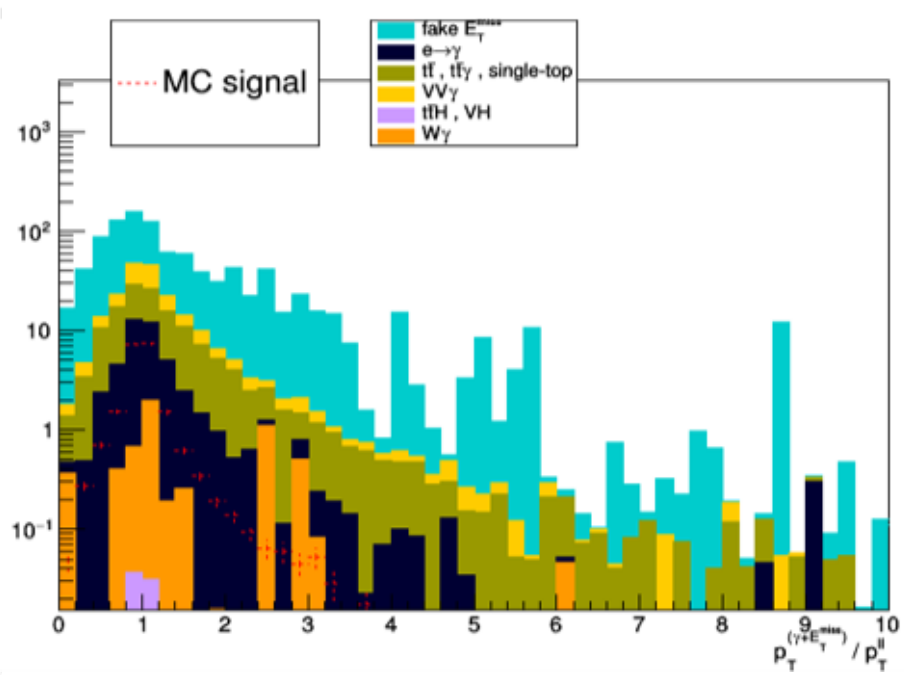

Leptons transverse momentum $\vec{p}_T^{ll}$

$$\vec{p}_T^{ll} = \vec{p}_T^{l1} + \vec{p}_T^{l2}$$

Figure 25: eeγ channel

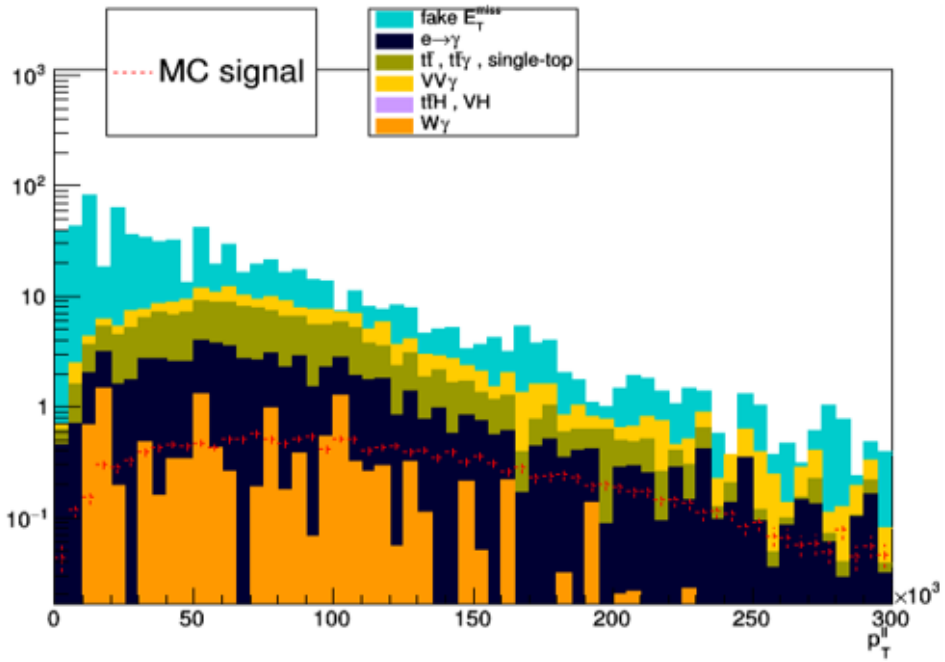

Figure 26: $\mu\mu\gamma$ channel

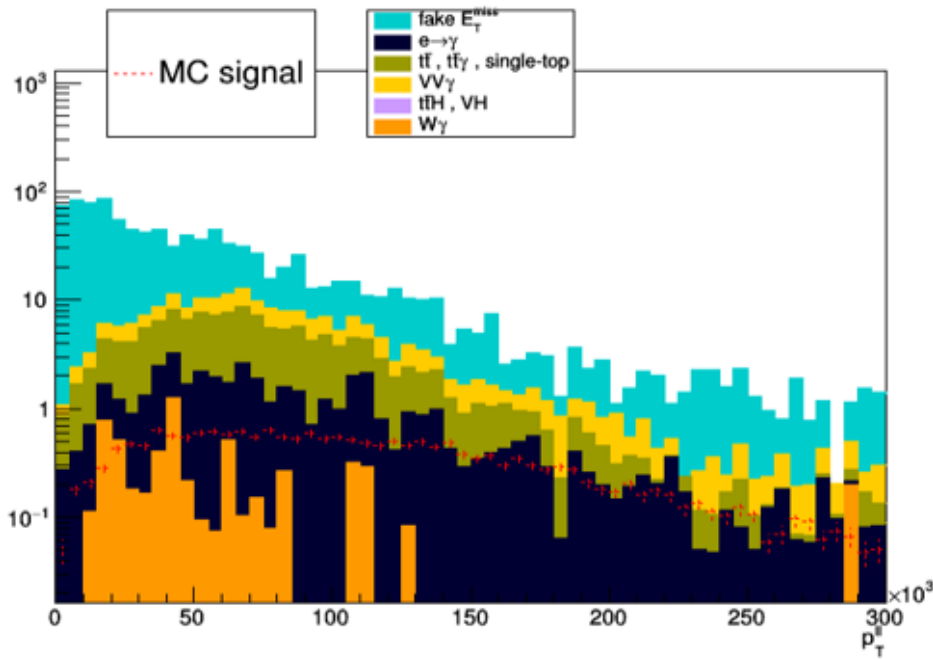

Photon transverse momentum $\vec{p}_T^{\,\gamma}$

Figure 27: eeγ channel

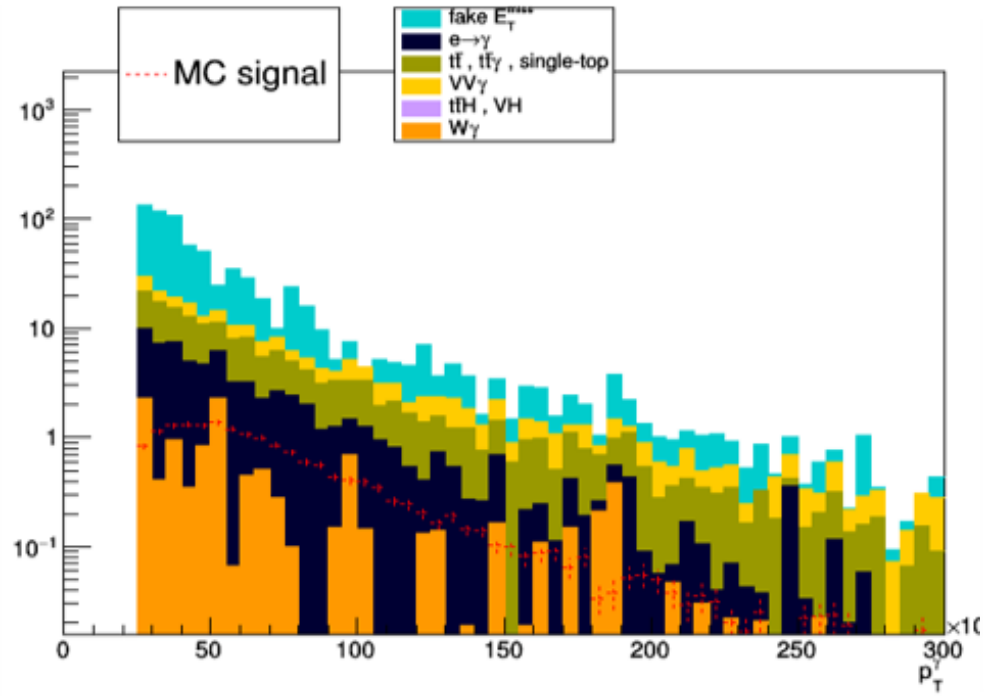

Figure 28: $\mu\mu\gamma$ channel

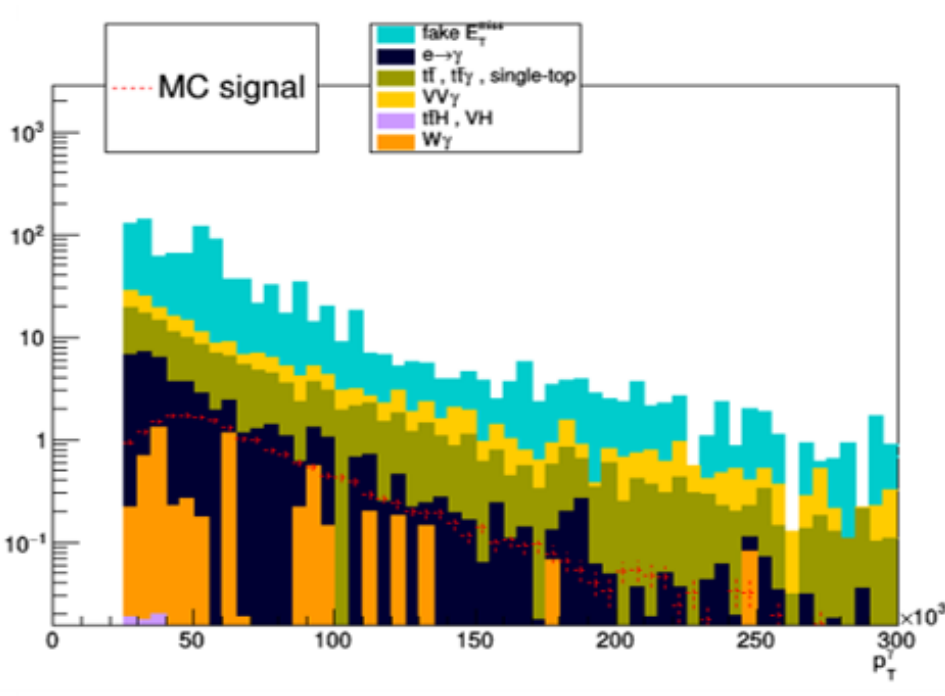

$p_T^{balance}$, $\vec{p}_T^{ll}$, $\vec{p}_T^{\gamma}$

Notes

- A peak is observed in $p_T^{balance}$ around 1 more evident for signal.
- There is a cut at $25\,\mathrm{GeV}$ in photon momentum $\vec{p}_T^{\gamma}$ which defines SR
- p_T^{γ} should have a peak around $\frac{m_H}{2}$ but it is not observed due to Z-momentum contribute

Selections: mll-peak, nobjets, MET-A, mT-all, metsig-all

- mll-peak: selection of interval $[76\,\mathrm{GeV}, 116\,\mathrm{GeV}]$ in leptons invariant mass, around Z boson mass
- nobjets: b-veto, selection of events without b-jets
- MET-A: selection of A region, at high MET and high $\Delta\Phi(\vec{E}_T^{miss}, \vec{p}_T^{\gamma ll})$
- mT-all: no selections in transverse mass
- metsig-all: no selections in MET significance

MET $\vec{E}_T^{miss}$

$$\vec{E}_T^{miss} = -\left[\sum_e \vec{p}_T^{(e)} + \sum_\mu \vec{p}_T^{(\mu)} + \sum_\gamma \vec{p}_T^{(\gamma)} + \sum_\tau \vec{p}_T^{(\tau)} + \sum_{jet} \vec{p}_T^{(jet)} + \sum_x \vec{p}_T^{(x)}\right]$$

Figure 29: eeγ channel

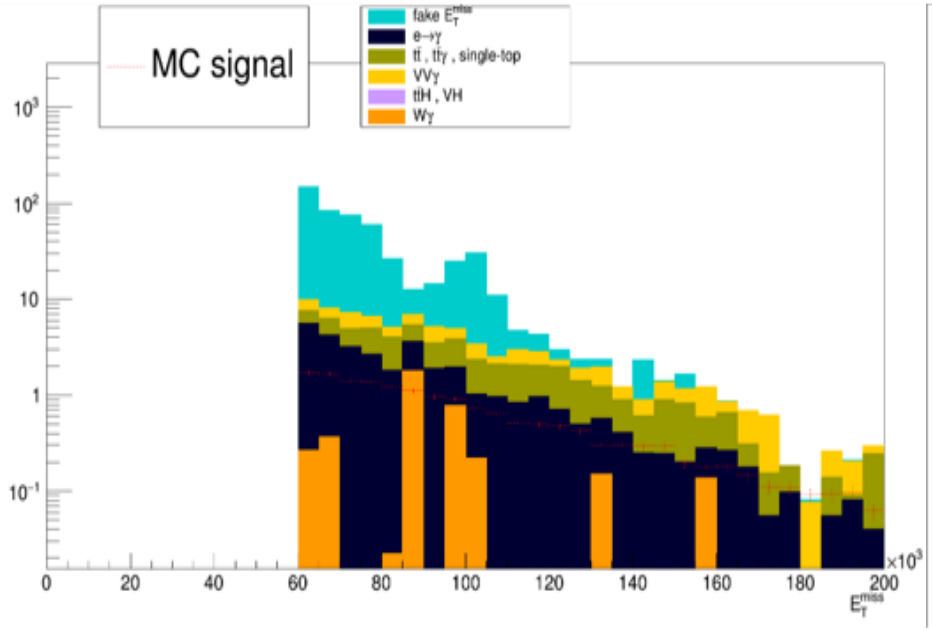

Figure 30: $\mu\mu\gamma$ channel

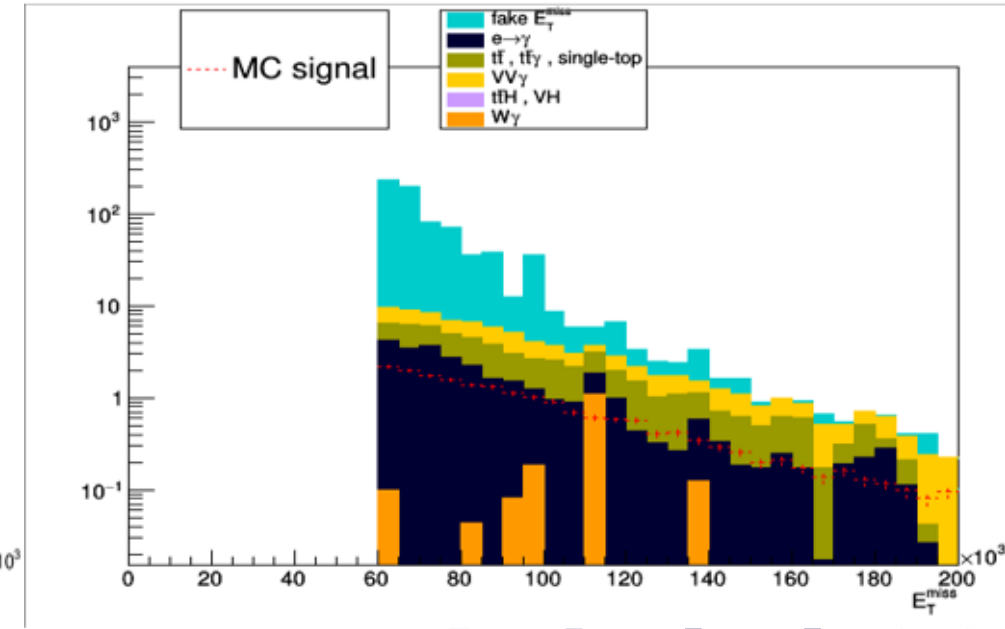

MET significance $\sigma_{E_T^{miss}}$

$$sig = \frac{E_T^{miss}}{\sigma_{E_T^{miss}}}$$

Figure 31: eeγ channel

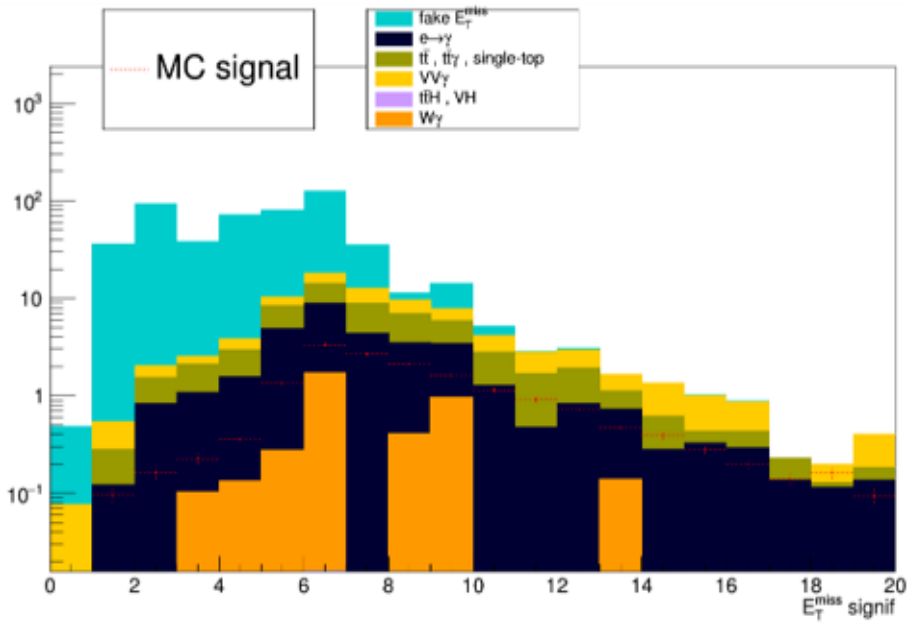

Figure 32: $\mu\mu\gamma$ channel

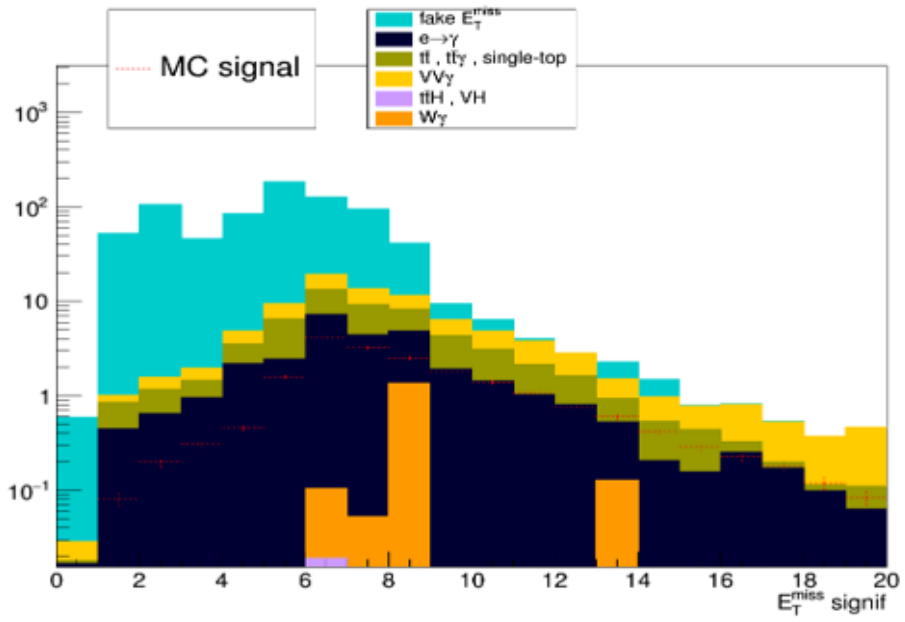

$\Delta\Phi(\vec{E}_T^{miss}, \vec{p}_T^{closest})$

Figure 33: eeγ channel

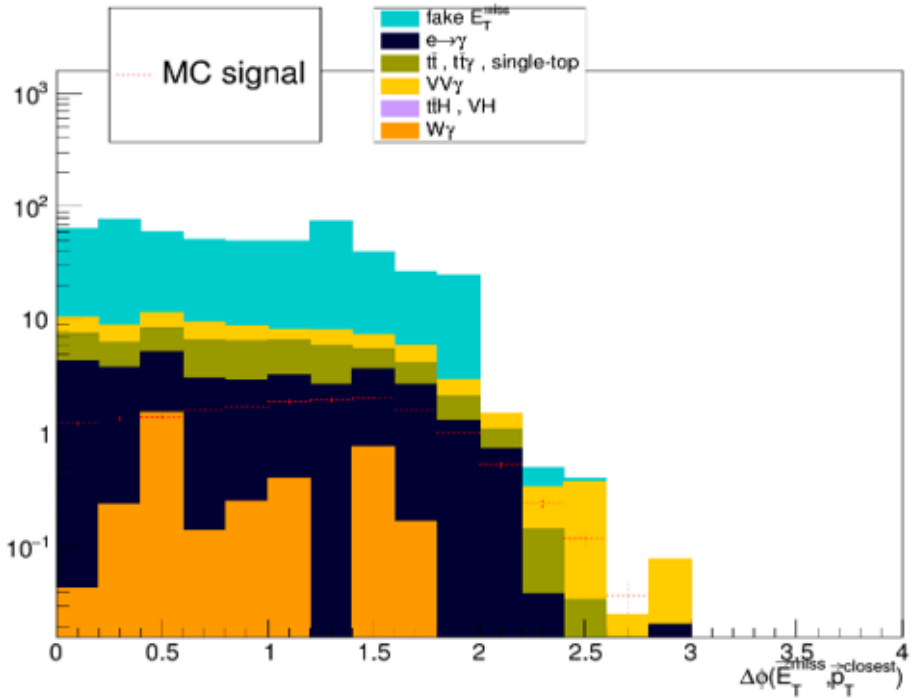

Figure 34: $\mu\mu\gamma$ channel

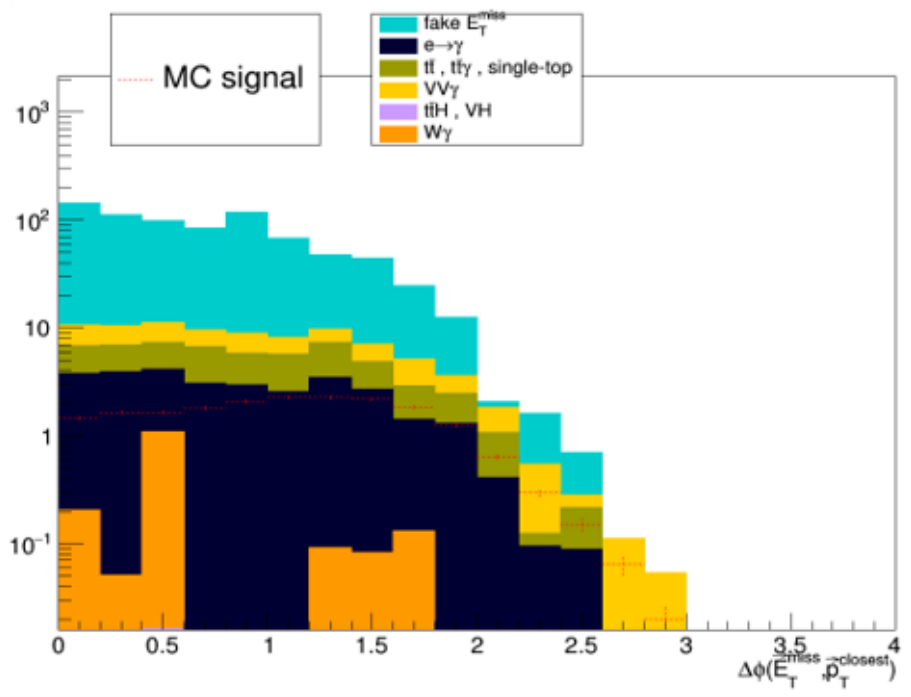

Invariant mass m_{ll}

$$m_{ll} = \sqrt{(E_{l1} + E_{l2})^2 - (\vec{p}_{l1} + \vec{p}_{l2})^2}$$

$$m_{ll} = \sqrt{2p_T^{l1}p_T^{l2}[\cosh(\eta^{l1} - \eta^{l2}) - cos(\Phi^{l1} - \Phi^{l2})]}$$

Figure 35: eeγ channel

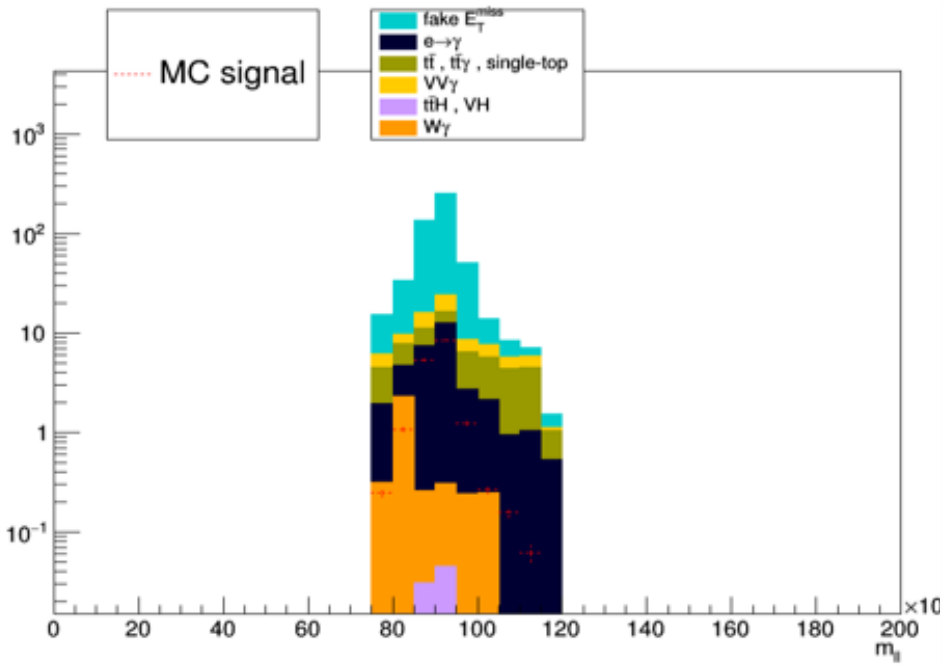

Figure 36: $\mu\mu\gamma$ channel

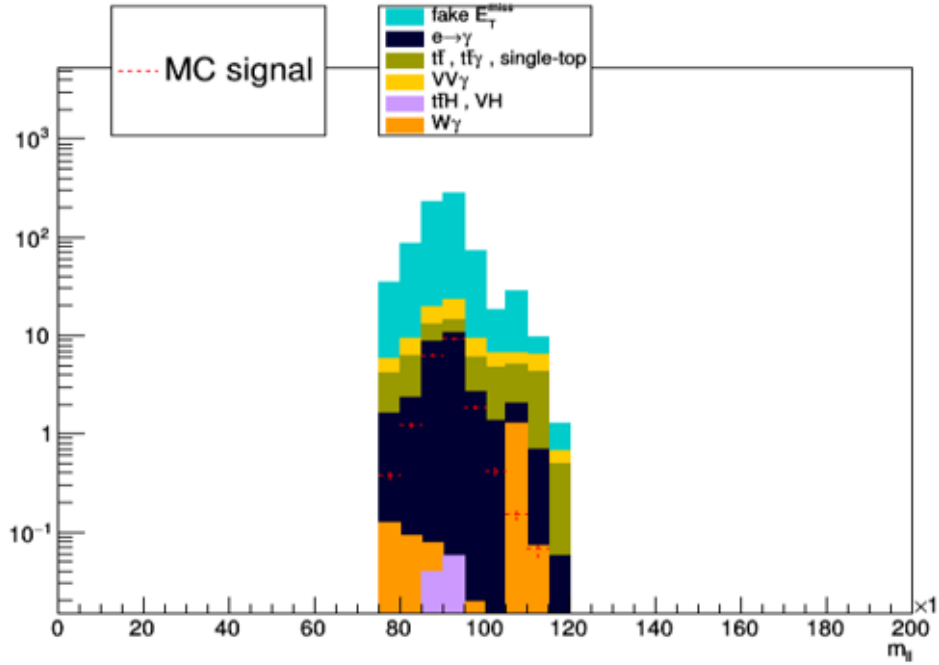

Other plots

- mll-all, mll-peak $[76\,\mathrm{GeV}, 116\,\mathrm{GeV}]$, mll-side $\notin [76\,\mathrm{GeV}, 116\,\mathrm{GeV}]$
- nobjets: b-veto, selection of events without b-jets
- MET-A: selection of A region, at high MET and high $\Delta\Phi(\vec{E}_T^{miss}, \vec{p}_T^{\gamma ll})$
- mT-all: no selections in transverse mass
- metsig-all: no selections in MET significance

Invariant mass m_{ll}

Figure 37: MET for different m_{ll} cuts

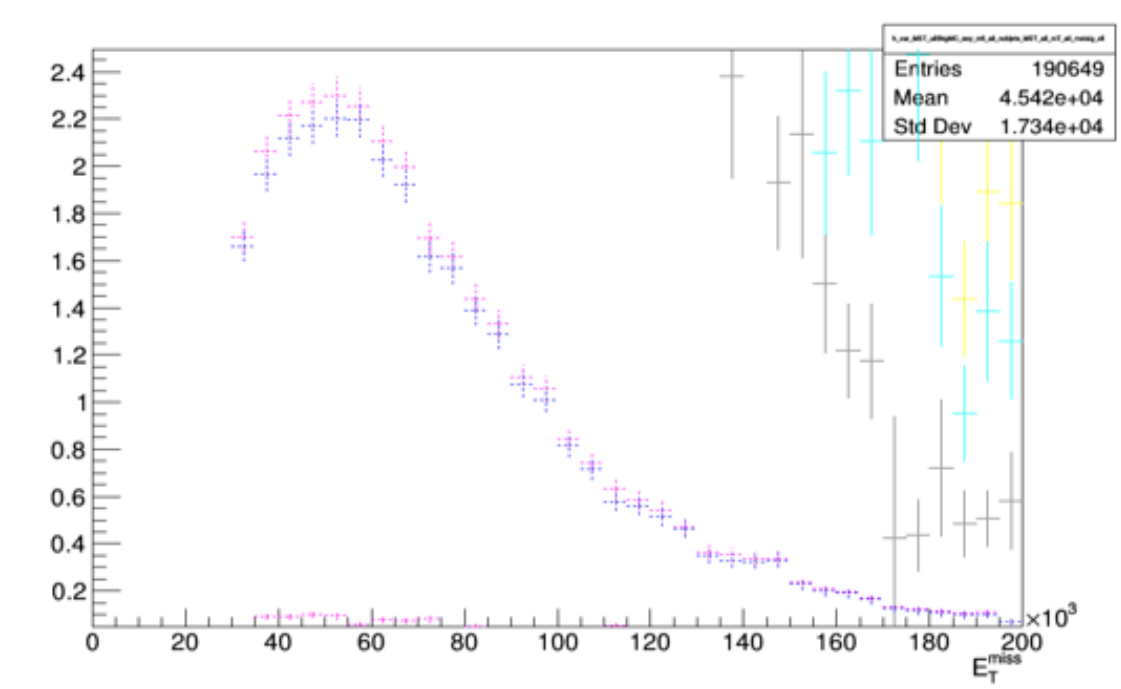

Blu and pink curves represents signal MET for m_{ll}-all, m_{ll}-peak and m_{ll}-side.
Yellow curve is background's MET for m_{ll}-all; light-blu curve for m_{ll}-peak and grey curve for m_{ll}-side.

Invariant mass m_{ll}

Figure 38: Signal's MET

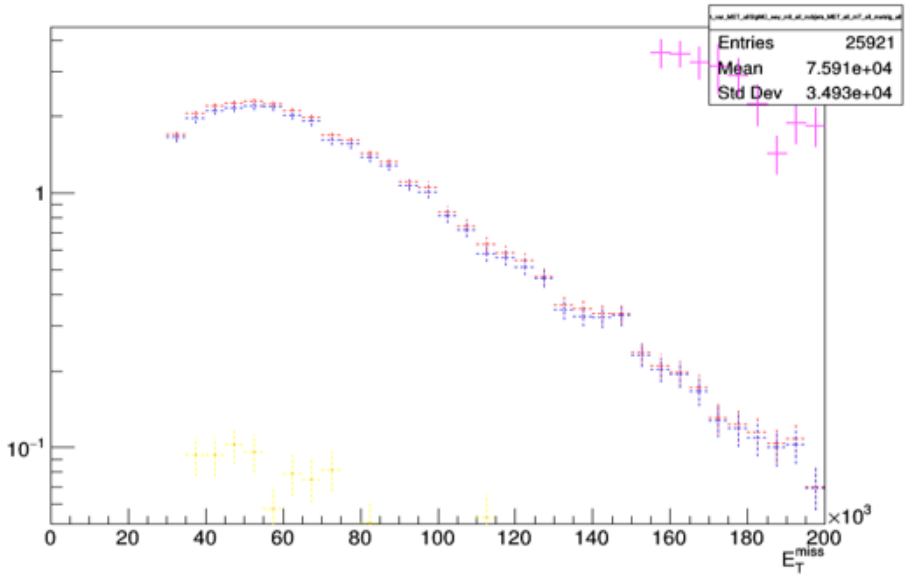

Figure 39: Background's MET

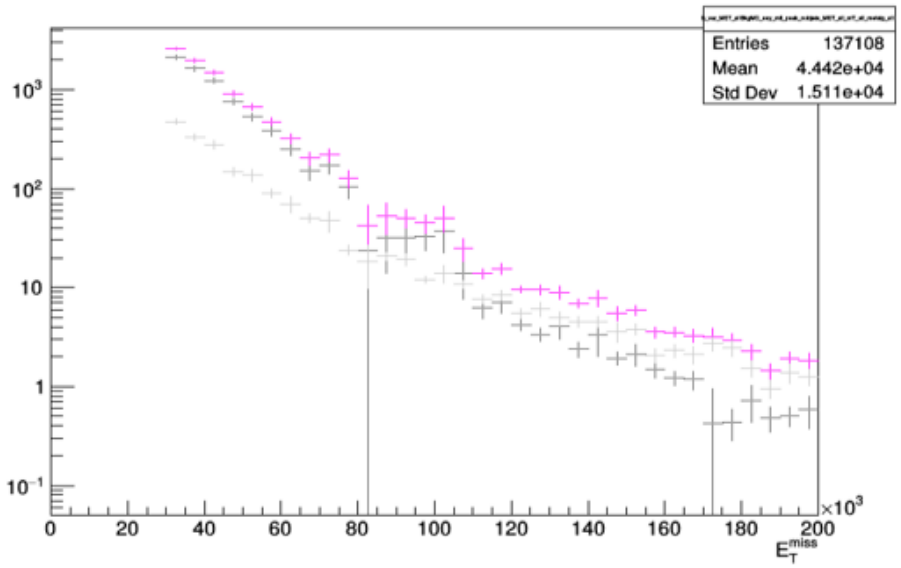

p_T balance

Figure 40: $p_T^{balance}$ for signal (red and yellow) and background (green and pink) in $\mu\mu\gamma$ and ee γ channels

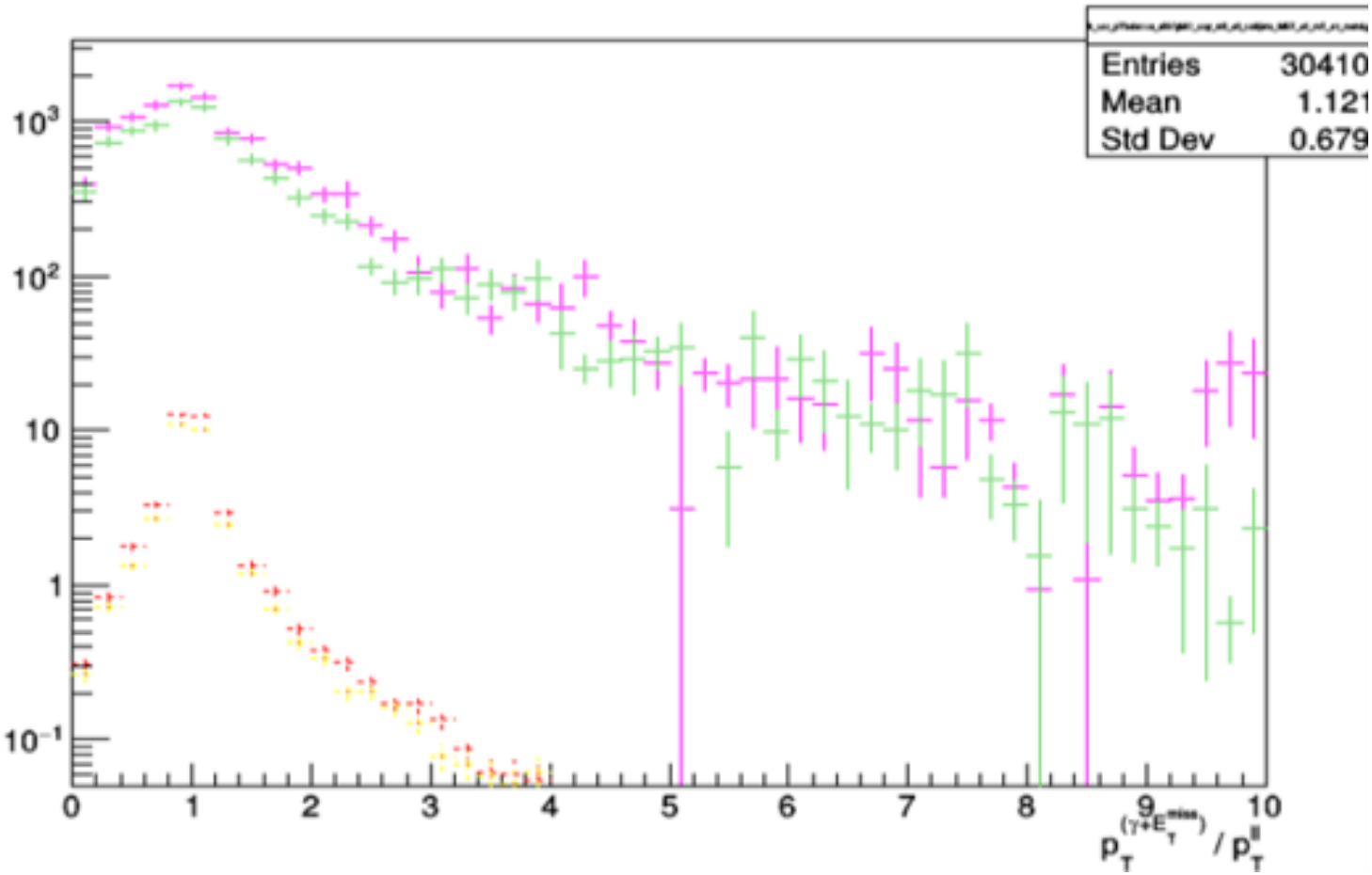

$\Delta\Phi(\vec{E}_T^{miss}, \vec{p}_T^{\gamma ll})$

Figure 41: $\Delta\Phi(\vec{E}_T^{miss}, \vec{p}_T^{\gamma ll})$ for signal (red and green) and background (yellow and grey) in $\mu\mu\gamma$ and eeγ channels

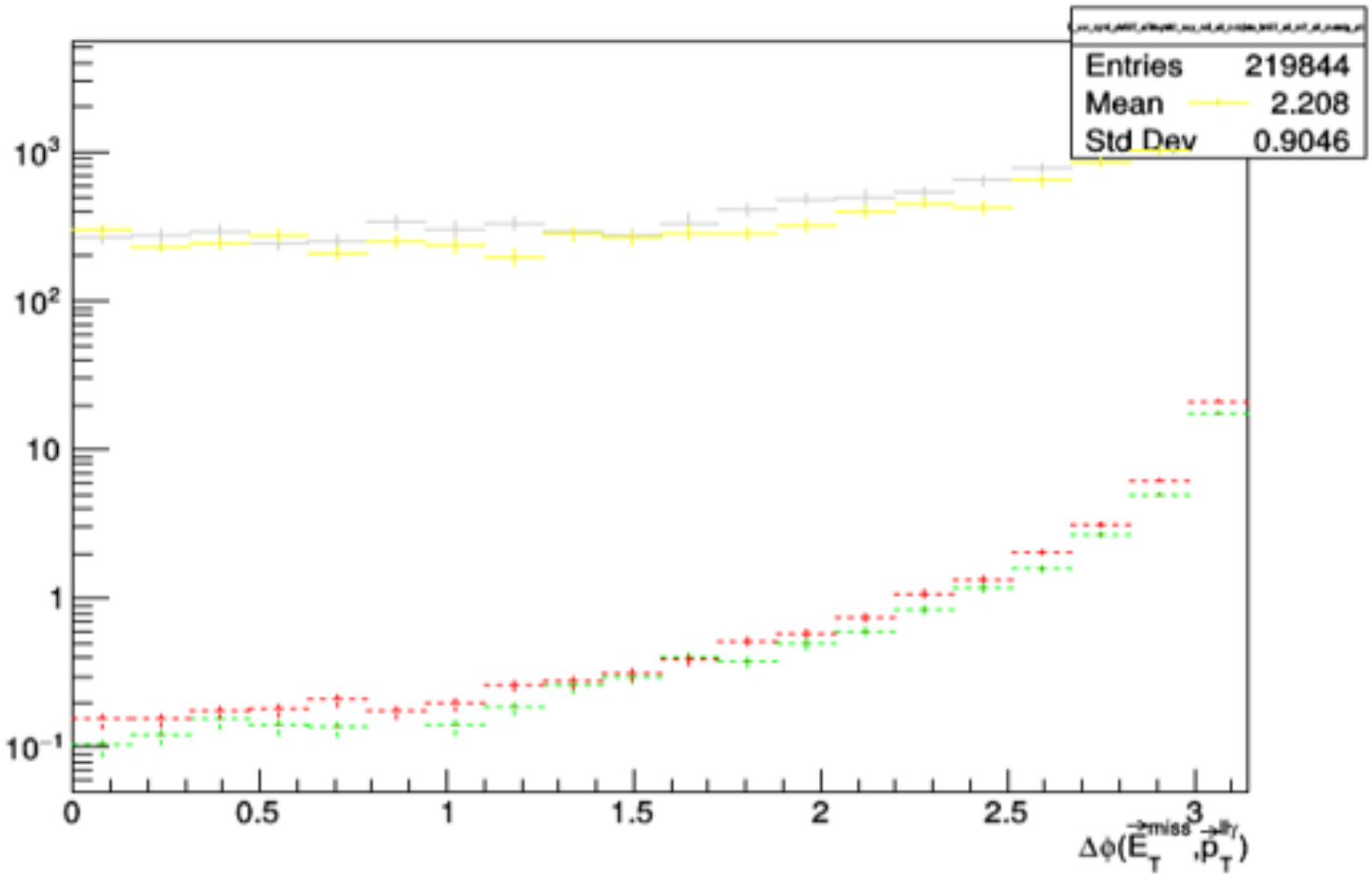

MET in A,B,C,D regions

Figure 42: Signal's MET in ABCD regions

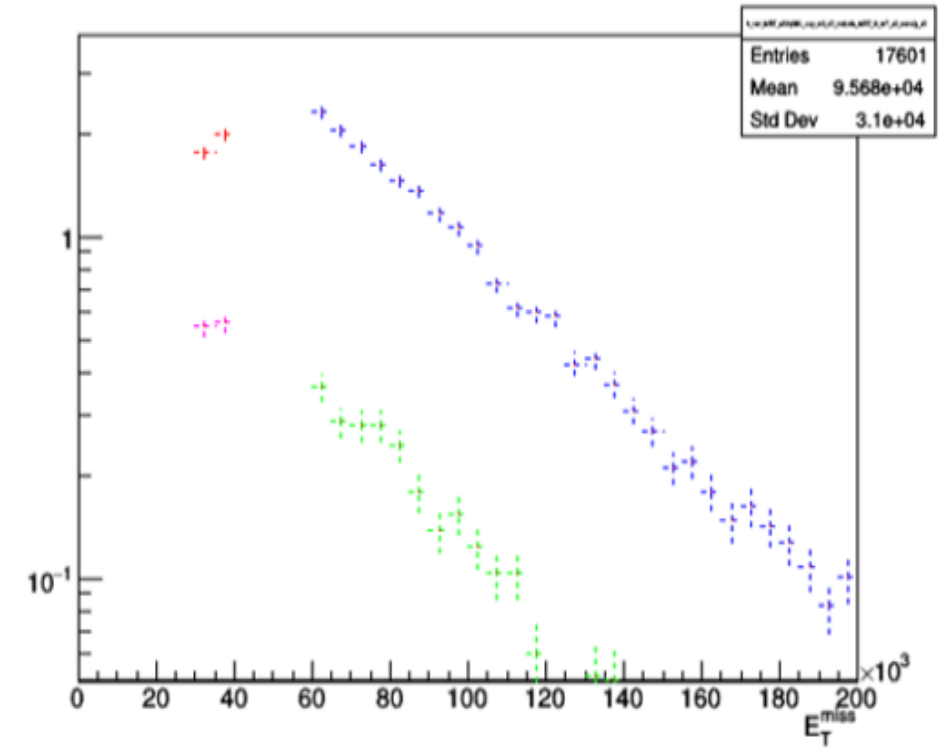

Figure 43: Background's MET in ABCD regions

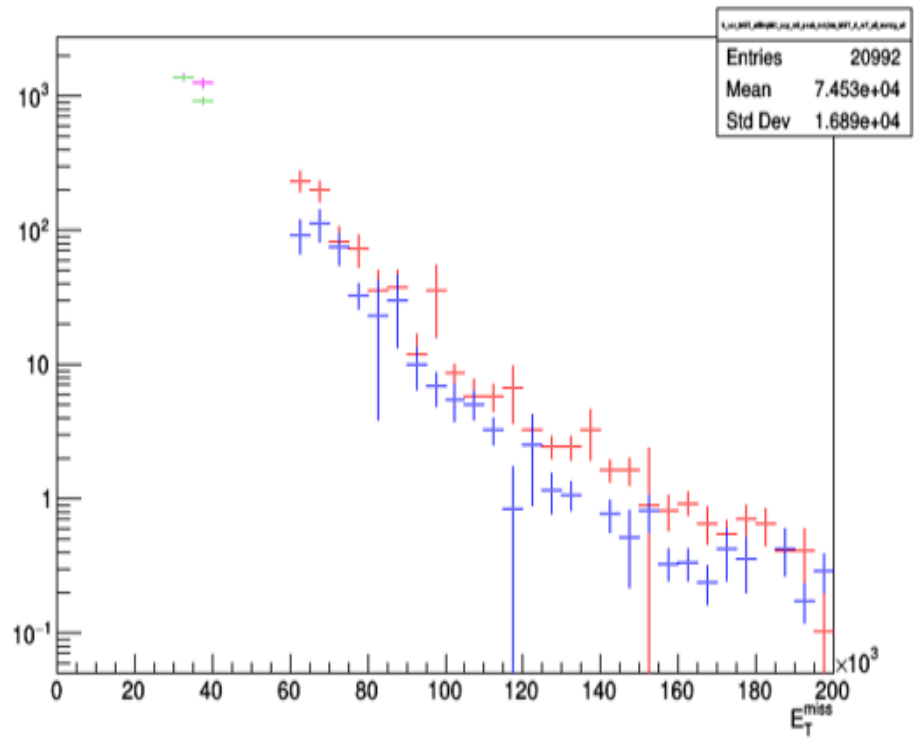

AOB